Esophageal cancer-related gene 4 is a secreted inducer of cell senescence expressed by aged CNS precursor cells

Yuki Kujuro[a,b], Norihiro Suzuki[b], and Toru Kondo[a,c,1]

[a]Laboratory for Cell Lineage Modulation, RIKEN Center for Developmental Biology, Kobe 650-0047, Japan; [b]Department of Neurology, Keio University School of Medicine, Tokyo 160-8582, Japan; and [c]Department of Stem Cell Biology, Ehime University Proteo-Medicine Research Center, Toon 791-0295, Japan

Edited by Hideyuki Okano, School of Medicine, Keio University, Tokyo, Japan, and accepted by the Editorial Board March 12, 2010 (received for review October 6, 2009)

Mammalian aging is thought to be partially caused by the diminished capacity of stem/precursor cells to undergo self-renewing divisions. Although many cell-cycle regulators are involved in this process, it is unknown to what extent cell senescence, first identified as irreversible growth arrest in vitro, contributes to the aging process. Here, using a serum-induced mouse oligodendrocyte precursor cell (mOPC) senescence model, we identified esophageal cancer-related gene 4 (*Ecrg4*) as a senescence inducer with implications for the senescence-like state of postmitotic cells in the aging brain. Although mOPCs could proliferate indefinitely when cultured using the appropriate medium (OPC medium), they became senescent in the presence of serum and maintained their senescent phenotype even when the serum was subsequently replaced by OPC medium. We show that *Ecrg4* was up-regulated in the senescent OPCs, its overexpression in OPCs induced senescence by accelerating the proteasome-dependent degradation of cyclins D1 and D3, and that its knockdown by a specific short hairpin RNA prevented these phenotypes. We also show that senescent OPCs secreted Ecrg4 and that recombinant Ecrg4 induced OPC senescence in culture. Moreover, increased Ecrg4 expression was observed in the OPCs and neural precursor cells in the aged mouse brain; this was accompanied by the expression of senescence-associated β-galactosidase activity, indicating the cells' entrance into senescence. These results suggest that Ecrg4 is a factor linking neural-cell senescence and aging.

cyclin D1 and D3 | neural precursor cells | oligodendrocyte precursor cells | retinoblastoma | senescence-associated β-galactosidase

Tissue-specific stem and precursor cells self-renew throughout the life of an animal and give rise to the many differentiated cells required for repairing damaged tissues. An age-related decline in the ability of these cells to self-renew (1–4) leads to a decreased ability to repair tissues and an increased incidence of degenerative diseases (5).

Cell senescence is defined as irreversible growth arrest, and it is provoked by a variety of stimuli, including DNA damage and telomere shortening. It acts as a potent barrier to tumorigenesis in vivo. However, whether cell senescence contributes to the decline of self-renewal in aged stem and precursor cells or the aging process in general is a matter of controversy (6, 7).

Oligodendrocyte precursor cells (OPCs) in the CNS differentiate into myelin-forming oligodendrocytes. OPCs persist in the adult brain and serve as a reservoir for new oligodendrocytes (8). Purified OPCs can be cultured indefinitely under appropriate conditions. In medium with a high serum concentration (e.g., 10%), however, they stop proliferating, become enlarged, and begin to express senescence-associated acidic β-galactosidase (SA-β-gal), a marker of cell senescence (9, 10). The ease of inducing these typical senescence phenotypes suggested that OPCs might serve as a model system for investigating the mechanisms of neural precursor cell senescence.

Recently, several secreted factors, such as insulin-like growth factor binding proteins (IGFBPs), IL, tumor growth factor-β (TGFβ), and plasminogen activator inhibitor 1 (PAI1), have been identified as senescence inducers (11–13). However, the factors involved in neural-cell senescence are largely unknown. Here, we show that esophageal cancer-related gene 4 (Ecrg4) is secreted and induces senescence in OPCs and neural precursor cells (NPCs) by a mechanism involving the proteasome-dependent degradation of cyclins D1 and D3. Moreover, we show that, in the aged brain, Ecrg4 expression increases in OPCs and NPCs and is accompanied by a high level of SA-β-gal activity. These findings show that Ecrg4 is a secreted factor for neural-cell senescence.

Results and Discussion

To study factors involved in neural-cell senescence, we first characterized senescence in OPCs. Purified mouse OPCs (mOPCs) had a bipolar shape and proliferated in OPC medium, which contained 0.25% FCS (low serum condition), but when cultured in medium with 10% FCS (high serum condition) for 10 days, the cells grew larger, became flatter (Fig. 1*A*), expressed SA-β-gal activity (Fig. 1*B*), and withdrew from the cell cycle (Fig. 1C). All of these characteristics were maintained when the cells were returned to low serum medium for another 10 days (reversion medium) (Fig. 1 *A*–*C*). In addition, the cell-cycle arrest was associated with sustained dephosphorylation of the retinoblastoma protein (Rb) (Fig. 1*D*). These features are typical of cell senescence (6, 7, 14–17). To exclude the possibility that cells' failure to reexpand was caused by an artifact of the anchored culture, we dissociated OPCs cultured in 10% FCS medium from the plate and expanded them in OPC medium in noncoated culture plates. The cells, however, soon attached to the plate and did not proliferate again, even after 10 days in culture (Fig. S1). Together, these data showed that OPCs become senescent at high serum concentrations.

To identify genes involved in OPC senescence, we compared the gene-expression profiles of senescent mOPCs grown in high serum or reversion medium with those of proliferating mOPCs using DNA microarrays. We found that 1,167 (clusters 1 and 2) and 622 (clusters 3 and 4) genes were up- or down-regulated in high serum, respectively, and 309 (cluster 2) and 199 (cluster 3) of the genes remained up- or down-regulated in the reversion medium, respectively (Fig. S2*A*). We confirmed the differential expression of a subset of the candidate senescence-associated

Author contributions: Y.K. and T.K. designed research; Y.K. and T.K. performed research; Y.K., N.S., and T.K. analyzed data; and Y.K. and T.K. wrote the paper.

The authors declare no conflict of interest.

This article is a PNAS Direct Submission. H.O. is a guest editor invited by the Editorial Board.

[1]To whom correspondence should be addressed. E-mail: tkondo@cdb.riken.jp.

This article contains supporting information online at www.pnas.org/lookup/suppl/doi:10.1073/pnas.0911446107/-/DCSupplemental.

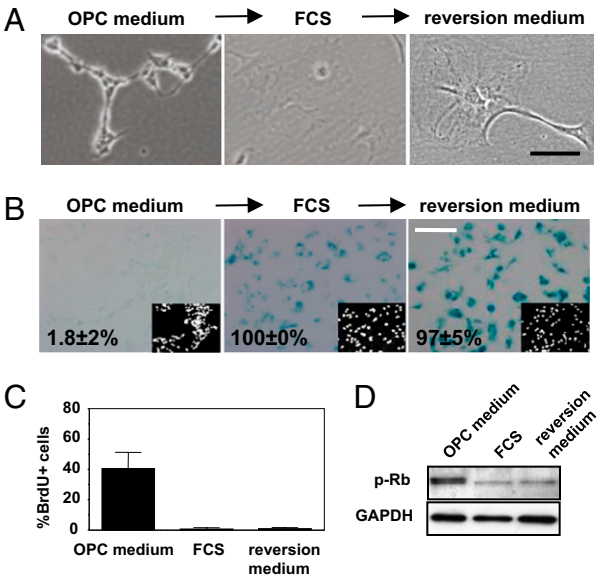

Fig. 1. A high concentration of FCS induces mOPC senescence. (*A*) Morphology of mOPCs cultured in low FCS, high FCS, and reversion medium. (Scale bar, 10 μm.) (*B–D*) Data from cells cultured as in *A*. (*B*) SA-β-gal staining of mOPCs. (Scale bar, 100 μm.) (*Insets*) DAPI staining (white) of the same field. (*C*) Percentage of BrdU+ mOPCs shown as the mean ± SD of three independent experiments. (*D*) Western blot analysis for phosphorylated Rb (p-Rb). GAPDH is a loading control.

genes by RT-PCR. This subset included RNA polymerase III polypeptide K (Polr3k), multiple EGF-like domain 9 (Megf9), ceruloplasmin (Cp), avian musculoaponeurotic fibrosarcoma (v-maf), As42 oncogene homolog (Maf), and *Ecrg4* [also known as RIKEN cDNA 1500015O10 or chromosome 2 ORF 40 (C2orf40)], all of which were ranked two times in the top-40 probe sets as determined by the false discovery rate (FDR) values in clusters 2 and 3 (Fig. 2*A* and Fig. S2 *B* and *C*). Of these, we focused on *Ecrg4* for three reasons. First, of the selected genes, *Ecrg4*'s mRNA level showed the largest difference between the senescent and nonsenescent OPCs (Fig. 2*A*). Western blotting and immunostaining confirmed the senescence-associated expression of the Ecrg4 protein (Fig. 2 *B* and *C*). Second, *Ecrg4* is down-regulated in various tumors (18) [Swedish Human Proteome Resource (HPR) program; http://www.proteinatlas.org/intro.php]. Third, *Ecrg4* was induced in senescent mouse embryonic fibroblasts (MEFs) cultured for a long time (passage 6) but not in MEFs at passage 1 (Fig. S3).

We next asked if *Ecrg4* is involved in OPC senescence. Because the efficiency of gene transfer into primary mOPCs is very low with the available methods, we used a rat OPC line, the Central Glia 4 (CG4), which has a normal karyotype and the potential to differentiate into oligodendrocytes (19). As shown in Fig. 2*D*, 40% of the CG4 cells transfected with an *Ecrg4* expression vector became SA-β-gal positive, whereas only 6% of the control vector-transfected cells became positive. Moreover, the overexpression of *Ecrg4* induced G1 arrest, dephosphorylation of Rb, and decreased expression of cyclins D1 and D3, which are essential regulators for the G1/S-phase transition (Fig. 2 *F–H*). In contrast, the knockdown of *Ecrg4* by a specific shRNA prevented these phenotypes in the CG4 cells cultured in OPC medium with 10% FCS (Fig. 2 *E–H*).

We also found that neither the overexpression nor the knockdown of *Ecrg4* affected the levels of cyclin-dependent kinases (CDKs) or CDK inhibitors; however, the addition of the proteasome inhibitor lactacystin blocked the ectopic Ecrg4-induced decrease in cyclins D1 and D3 (Fig. 2*I*), suggesting that the reduced level of these cyclins was caused by their degradation, as shown previously for the F-box protein 31 (FBXO31), which induces G1 arrest after DNA damage through cyclin D1 degradation (20). Consistent with these results, we observed that the overexpression of Ecrg4 did not affect the levels of cyclin D1 or D3 mRNA (Fig. 2*J*). Together, these results indicated that Ecrg4 induces OPC senescence in part by reducing cyclins D1 and D3 and by dephosphorylating Rb.

To investigate the Ecrg4 protein domains responsible for inducing cell senescence, we constructed a panel of Ecrg4 deletion mutants, including one in which the N-terminal signal peptide was deleted (the Signal– mutant; schematic diagrams in Fig. S4*A Left*). As shown in Fig. S4, none of the deletion mutants induced senescence, suggesting that only the secreted full-length form of Ecrg4 is functional. Indeed, we identified Ecrg4 in the culture medium of senescent mOPCs (Fig. 3*A*) and showed that, after the expression of *Ecrg4* or *Ecrg4* shRNA in CG4 cells, the level of Ecrg4 in the culture medium increased or decreased, respectively (Fig. S5*B*). Moreover, we found that the addition of recombinant mouse Ecrg4 (rEcrg4), which was generated by the baculovirus-infected silkworm system (21), induced mOPCs to become senescent: the cells expressed SA-β-gal activity, lost cyclins D1 and D3 expression, and withdrew from the cell cycle (Fig. 3 *B–D*). In addition, we found that the senescent OPCs induced by rEcrg4 were positive for oligodendrocyte O antigen 4 (O4), a marker for OPCs, but not for GFAP, a marker for astrocytes that is induced by the addition of high FCS, revealing that the Ecrg4-induced OPC senescence was not the result of the OPCs becoming either astrocytes or oligodendrocytes (Fig. 3*E*). We also found that rEcrg4 induced senescence in CG4 cells (Fig. S6 *C* and *D*) and MEFs (Fig. S6 *E–G*). Together, these results showed that Ecrg4 is a secreted inducer of cell senescence.

To investigate if *Ecrg4* might be involved in aging, we examined its expression in the brain of the adult mouse. Although the expression of *Ecrg4* was low in the brains of young, 2-month-old adult mice (except for the mitral cell layer of the olfactory bulb), it was strongly expressed in the brains of aged, 15- to 21-month-old mice in the subgranular zone (SGZ) of the dentate gyrus where NPCs reside, in the corpus callosum (CC) where OPCs are abundant, and in the CA1-3 regions of the hippocampus, cerebellum, brainstem, and cortex where neurons are dominant (Fig. 4*A*).

To confirm if OPCs and NPCs express Ecrg4 in the brain of aged mice, we immunolabeled brain sections for Ecrg4 and either the OPC markers Olig1 and NG2 or the NPC markers Musashi1 and Sox2 (22, 23). We found that most of the Ecrg4+ cells in the CC were Olig1+ (80%) and NG2+ (64%) (Fig. 4*B*) and that a large fraction of the Ecrg4+ cells in the SGZ were Musashi1+ (89%) and Sox2+ (59%) (Fig. 4*D* and Fig. S7 *A* and *B*). In contrast with their nuclear localization in the young brain (Fig. 4 *B* and *D*), we observed cytoplasmic localization of Olig1 and Sox2 in the aged brain, and the immunolabeling signals for these proteins were eliminated when the antibodies were preincubated with recombinant Sox2 (rSox2) or recombinant Olig1 (rOlig1) (Fig. S7 *C* and *D*). Because the Olig1 and Sox2 localizations are regulated by nucleo-cytoplasmic shuttling under the control of importin and exportin (24, 25), the shift of these transcription factors from the nucleus to the cytoplasm may reflect an age-dependent decline in nuclear pore activity (26–28). Moreover, we found that many cells in the CC (Fig. 4*C*) and SGZ (Fig. 4*E*) were positive for SA-β-gal. Double labeling revealed that all of the SA-β-gal-positive cells expressed Ecrg4 (Fig. 4*F*) and that the Ecrg4+ cells in the aged brain did not incorporate BrdU (Fig. S8). Collectively, these data suggested that Ecrg4 is up-regulated in the OPCs of the aged CC and the NPCs of the aged SGZ, both of which are entering senescence.

The findings that NPCs in the aged SGZ express Ecrg4 and are positive for SA-β-gal led us to examine primary cultures of hippocampal NPCs to determine if their overexpression of Ecrg4 or the addition of rEcrg4 to the cultures could induce the cells to

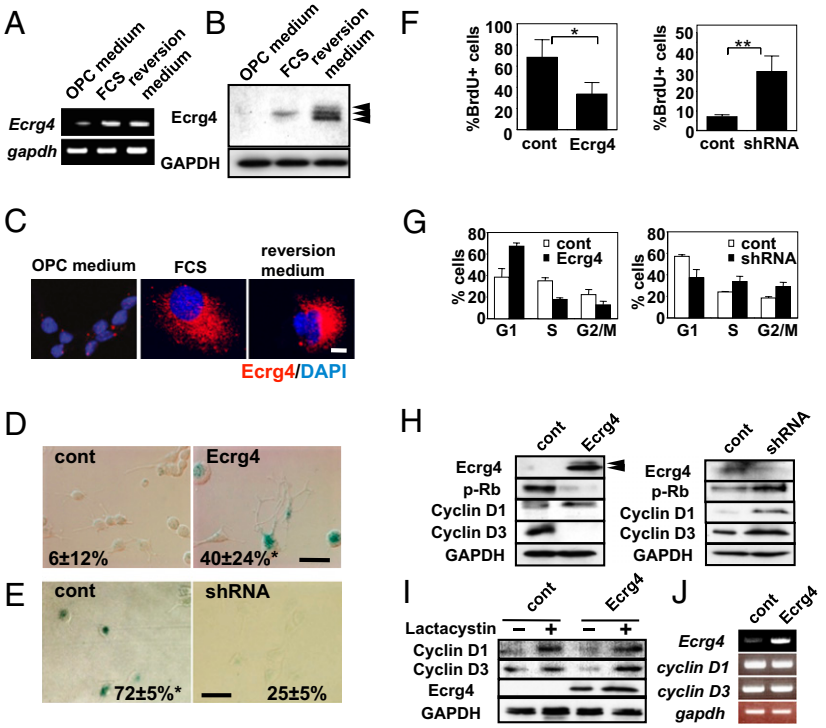

Fig. 2. *Ecrg4* induces senescence accompanied by the proteasomal degradation of cyclins D1 and D3. (*A–C*) Ecrg4 expression in mOPCs cultured in low FCS, high FCS, and reversion medium and analyzed by RT-PCR (*A*), Western blotting (*B*), and immunolabeling (C). (Scale bar, 10 μm.) Arrowheads in *B* indicate bands with probable protein modifications. (*D* and *E*) SA-β-gal staining (green) of CG4 cells overexpressing either *Ecrg4* (*D*) or *Ecrg4*-shRNA (*E*). (Scale bar, 50 μm.) (*F*) Percentage of BrdU+ CG4 cells overexpressing *Ecrg4* (*Left*) or *Ecrg4*-shRNA (*Right*). (*G*) Cell-cycle analysis of CG4 cells overexpressing *Ecrg4* (*Left*) or *Ecrg4*-shRNA (*Right*). (*H*) Western blot analysis of cell-cycle regulatory proteins in CG4 cells overexpressing *Ecrg4* (*Left*) or *Ecrg4*-shRNA (*Right*). (*I*) Levels of cyclin D1 and D3 in Ecrg4-overexpressing CG4 cells with or without lactacystin. (*J*) RT-PCR analysis of cell-cycle regulatory proteins in *Ecrg4*-expressing CG4 cells. $*P < 0.05$ and $**P < 0.01$ compared with control. Values denote the mean ± SD of three independent experiments.

become senescent. As shown in Fig. S9 *A–F*, both treatments induced hippocampal NPC senescence. In addition, we confirmed that the knockdown of Ecrg4 by shRNA blocked the induction of senescent phenotypes in the hippocampal NPCs by 10% FCS (Fig. S9 *G–I*). Together, these findings suggested that Ecrg4 is also involved in NPC senescence in the aged SGZ in vivo.

A more detailed analysis of Ecgr4 expression in vivo revealed that, in the aged brain, not only precursor cells but also neurons, including granule cells in the hippocampus (Fig. S10*A*), Purkinje cells in the cerebellum (Fig. S10*B*), and NeuN+ cells in the brainstem (Fig. S10*C*), expressed Ecrg4 at higher levels than in the young brain. A comparison between sections stained for Ecgr4 and SA-β-gal showed that cells with the same morphology and location were labeled by both markers (Fig. S10*D*). This finding was surprising, because cell senescence is not thought to occur in cells that have already withdrawn from the cell cycle, like neurons, and further investigation is required to understand why these cells showed the senescent phenotype (7).

Here, we showed that *Ecrg4* is a secreted senescence inducer expressed in aged OPCs and NPCs. However, we did not find clusters of Ecrg4+ cells in the aged brain, indicating that neighboring cells do not become senescent at one time, perhaps owing to unknown inhibitors for Ecrg4 or Ecrg4 acting in a cell-autonomous manner, as in the case of IL6 (29). Nonetheless, because other senescence-inducing secretion factors (30), including IGFBPs, IL, TGFβ, and PAI1, not only induce senescence but also cause or contribute to degenerative changes in the surrounding cells (31–33), it will be of great interest to investigate the physiological significance of Ecrg4's function. Additionally, it will be interesting to learn if its inhibition delays the processes of brain aging and if Ecrg4 contributes to differences between fetal/neonatal and adult OPCs in myelination speed and competence, as previously shown by Windrem et al. (8), although Ecrg4 is unlikely to be involved in oligodendrocyte differentiation (Fig. 3*E*).

Materials and Methods

Animals and Chemicals. The mice were obtained from the Laboratory for Animal Resources and Genetic Engineering at the RIKEN Center for Developmental Biology (CDB) and Charles River. The mice used as young adults were 2-months old, and aged mice were 15- to 21-months old. All of the mouse experiments were performed following protocols approved by the RIKEN CDB Animal Care and Use Committee. Chemicals and growth factors were purchased from Sigma and Peprotech, respectively, except where indicated.

OPC Culture. The mOPCs were prepared from the telencephalic neuroepithelial cells of embryonic day 14.5 mice and purified by sequential immunopanning, as described previously (34). Purified mOPCs and the CG4 line were maintained in OPC medium, which consisted of DMEM containing chemicals, PDGFAA (10 ng/mL) and bFGF (2 ng/mL) along with 0.25% FCS (low serum condition) (9), except where indicated. DMEM lacking the other supplements and with 10% FCS (high serum condition) was used to induce the senescence of mOPCs. The shRNA experiments were performed in OPC medium, but the FCS was increased to 10% or 0.75%.

Cloning of Mouse Ecrg4 cDNA and Construction of Deletion Mutants. Full-length mouse *Ecrg4* (m*Ecrg4*) and rat *Ecrg4* were amplified from the cDNA of senescent mOPC and CG4 cells, respectively, using RT-PCR and Phusion polymerase (Finnzyme), and they were cloned into the pDrive vector (Qiagen) following the manufacturer's instructions. Deletion mutants of m*Ecrg4* [dC1 containing amino acid residues (AA) 1–100; dC2 containing AA 1–50; Signal–containing AA 32–147; dN1 lacking AA 32–50; and dN2 lacking AA 32–100] were constructed by PCR and sequenced using the BigDye Terminator Kit version 3.1 (Applied Biosystems) and an ABI sequencer (model 3130xl; Applied Biosystems).

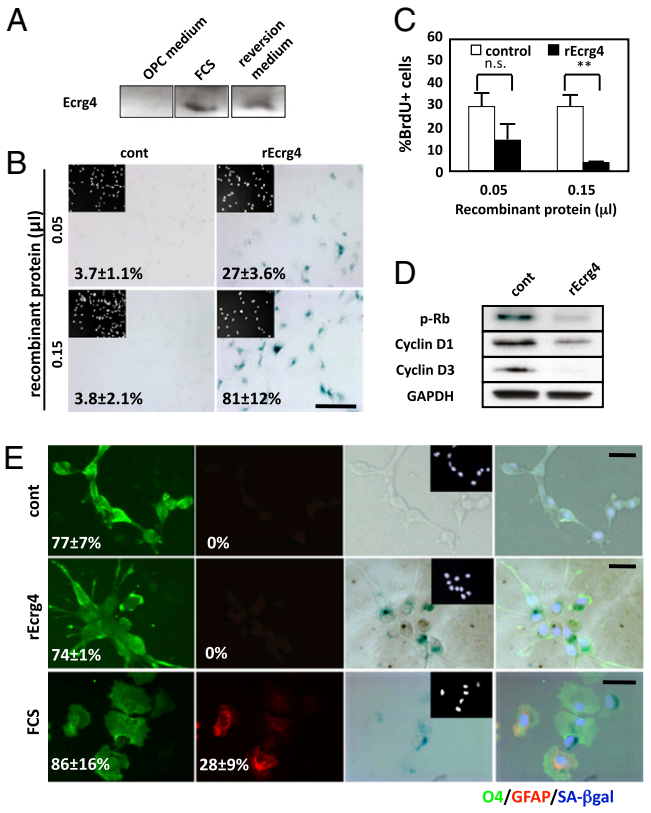

Fig. 3. Ecrg4 is secreted, and recombinant Ecrg4 protein induces senescence in mOPCs. (*A*) Immunoblot analysis of the culture medium from mOPCs grown in all three conditions and probed for Ecrg4. (*B–D*) Experiments were performed with mOPCs treated with rEcrg4 or a control cell extract. (*B*) SA-β-gal staining. (Scale bar, 100 μm.) (*C*) Percentage of BrdU+ mOPCs. (*D*) Immunoblot analysis of p-Rb, cyclin D1, and cyclin D3. (*E*) Costaining of SA-β-gal, O4, and GFAP in either rEcrg4- or FCS-treated senescent OPCs. (Scale bar, 50 μm.) $^{**}P < 0.01$ compared with control. ns, not significant. Values denote the mean ± SD of three independent experiments.

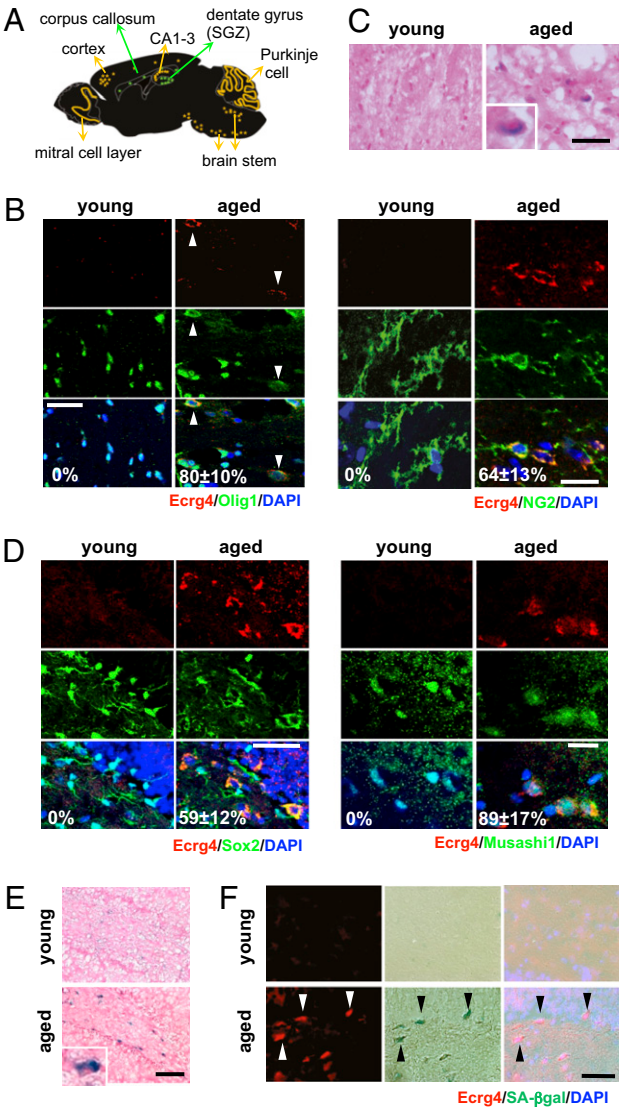

Fig. 4. Increased expression of Ecrg4 in senescent NPCs and OPCs in the aged mouse brain. (*A*) Schematic diagram showing the location of Ecrg4+ cells in the brain of aged (15–21 months old) mice. Green, NPCs and OPCs; yellow, neurons. (*B–F*) Comparison of the labeling for various markers in the brain of young (2 months old) and aged mice. (*B*) Immunolabeling of the CC for Ecrg4 and Olig1 (*Left*) or Ecrg4 and NG2 (*Right*). (Scale bar, 30 μm.) (*C*) SA-β-gal staining (blue) of the CC that is counterstained with Nuclear Fast Red (pink). (Scale bar, 30 μm.) (*D*) Immunolabeling of the dentate gyrus for Ecrg4 and Sox2 (*Left*) or Ecrg4 and Musashi1 (*Right*). (Scale bar, 50 μm.) (*E*) SA-β-gal staining (blue) of the dentate gyrus as in *C*. (Scale bar, 100 μm.) (*F*) Colocalization of SA-β-gal (green) and Ecrg4 (red) in the aged dentate gyrus. (Scale bar, 50 μm.) Arrowheads point to Ecrg4+SA-β-gal+ cells. All nuclei were counterstained with DAPI (blue).

The following oligonucleotide DNA primers were synthesized to amplify full-length m*Ecrg4*: forward, 5′-AACGCGTGCCACCATGAGCACCTCGTCTGCGCG-3′; reverse, 5′-TCTCGAGTTAATAGTCATCATAGTTGACACT-3′. The m*Ecrg4* forward primer was paired with these reverse primers: 5′-TCTCGAGATCATCTTCAAATTTAGCCTCATC-3′ for dC1 and 5′-TCTCGAGATTAGTCTTTGACGGGACAGGT-3′ for dC2. The m*Ecrg4* reverse primer was paired with 5′-TGGATCCGCCACCATGAACAAACTCAAGAAGATGCTC-3′ for Signal–, 5′-CATAAGTGGAGTAGCTGTAGCCGAGAAC-3′ for dN1, and 5′-CATAAGTGGAGTCAACTATTGGCTAAACAG-3′ for dN2. The primers for rat *Ecrg4* were forward, 5′-AGGATCCGCCACCATGGGCACCTCCTCTGCTCG-3′ and reverse, 5′-TCTCGAGATAGTCATCATAGTTGACACTGG-3′.

Vectors and Transfection. The m*Ecrg4* cDNA was inserted into pEFBOS-EX (S. Nagata, Kyoto, Japan), pCMS-EGFP, and pcDNA3 2×cFLAG to generate Ecrg4 fused with two tandem FLAG epitopes at its C-terminal end and pMO1 to generate the recombinant protein (Katakura Industries). Rat *Ecrg4* cDNA was inserted into pcDNA3 2×cFLAG. The resulting constructs were called pEFBOS-m*Ecrg4*, pCMS-EGFP-m*Ecrg4*, pcDNA3-m*Ecrg4* 2×cFLAG, pMO1-m*Ecrg4*, and pcDNA3-rat *Ecrg4* 2×cFLAG, respectively. Each m*Ecrg4* deletion mutant fragment was inserted into pcDNA3 2×cFLAG. The shRNA expression vector for *Ecrg4* (*Ecrg4*-shRNA; GATGAGGCTAAATTTGAAGAT) was purchased from SuperArray.

Transfections were performed using the Nucleofector procedure following the supplier's instructions (Amaxa). The transfected cells were selected in puromycin (0.25 μg/mL) for 2–4 days.

Recombinant Ecrg4 Protein. Recombinant mouse Ecrg4 (rEcrg4) protein was generated by the KaikoExpress Service (Katakura Industries Co. Ltd). In brief, silkworm larvae were inoculated with a recombinant baculovirus bearing the m*Ecrg4* cDNA, and the hemolymph was collected after several days. The hemolymph was precipitated with 10% polyethylene glycol by centrifugation (100,000 *g* for 1 h), and the supernatant (rEcrg4) was used for the experiment. The rEcrg4 appeared on Western blots (Fig. S6 *A* and *B*) as bands of ~14, 17, and 34 kDa. Because the molecular weights of mature Ecrg4 and its precursor are about 14 and 17 kDa, respectively, the 34-kDa protein was probably a dimer of uncleaved Ecrg4.

The mOPCs or CG4 cells were plated on Poly-D-Lysine–coated eight-chamber slides containing 500 μL of OPC medium. The rEcrg4 or a control protein (hemolymph supernatant collected from control vector-infected silkworms) was added, and the cells' SA-β-gal activity, BrdU incorporation, and differentiation status were evaluated 7 days later. mOPCs cultured in 10% FCS for 10 days served as a positive control for the anti-GFAP antibody.

Microarray Hybridization and Data Processing. The total RNA (100 ng) in each of two independent experiments was isolated and amplified using the Two-Cycle cDNA Synthesis Kit and in vitro transcription (IVT) Labeling Kit (Affymetrix). The cRNA was subsequently fragmented and hybridized to the GeneChip Mouse Genome 430 2.0 array (Affymetrix), according to the manufacturer's instructions. The microarray image data were processed with the GeneChip Scanner 3000 (Affymetrix) to generate cell library (CEL) data, which were summarized and normalized using the Robust Multichip Average (RMA) algorithm to compute the expression values (35). Statistical significance was determined by the eBayes method (36). The FDR was calculated, and probe sets showing an FDR <0.05 were selected as significantly different.

Immunoblot Analysis and Silver Staining. Western blot analyses of whole-cell extracts and rEcrg4 were performed using standard methods. Where indicated, 1 μM lactacystin (Calbiochem) was added for 48 h before preparing the protein extract. To prepare conditioned medium (CM), cells were grown in OPC medium, FCS, or OPC reversion medium, and the media were harvested and concentrated using Amicon Ultra tubes (10 k; Millipore). All of the media were changed 3 days before harvest. CM was normalized to the protein concentration of the cells before loading the gel.

Silver staining was performed using a SilverQuest Silver Staining kit (Invitrogen) following the manufacturer's instructions.

Immunohistochemical Analysis. Mouse brains were fixed in 4% paraformaldehyde at 4 °C overnight. After fixation, the brains were cryoprotected with 12–18% sucrose in PBS, embedded in Tissue-Tek Optimal Cutting Temperature (OCT) compound (Miles), and frozen. Sagittal sections (10 μm thick) were cut and stained for Ecrg4 and neural markers using standard techniques. Fluorescence images were obtained using a Fluoview FV1000 confocal laser-scanning microscope (Olympus). The recombinant mouse Sox2 protein (rSox2) was a gift from H. Aburatani (Tokyo, Japan), and recombinant mouse Olig1 (rOlig1) was generated using the pGEX4T2-mOlig1 vector (H. Takebayashi, Kumamoto, Japan) and a RediPack GST Purification module (GE Healthcare) following the manufacturer's instructions. In some experiments, the recombinant proteins (1 ng/μl) were preincubated with their specific antibodies for 1 h before immunostaining.

Proliferation and SA-β-gal Assays. To examine cell proliferation, the cells were labeled with BrdU (10 μM) for 6 h, fixed, and stained for BrdU as previously described (37). To quantify cell proliferation in the dentate gyrus, mice were given i.p. injections of 100 mg/kg BrdU three times per day for 3 days, and they were killed 5 days after the last injection. Brain-tissue sections were prepared as described above and stained for BrdU and Ecrg4 using standard protocols. Fluorescence images were obtained by using an Axio Imager A1 microscope (Carl Zeiss).

The SA-β-gal activity in cultured cells and brain sections was determined using a Senescence Detection Kit (Calbiochem) following the manufacturer's instructions. The images were obtained with an Axioplan 2 imaging microscope (Carl Zeiss).

Flow Cytometry. Cells were harvested and fixed as a single-cell suspension in 70% ethanol at −20 °C. The cells were recovered by centrifugation, stained with propidium iodide (Molecular Probes), and subjected to analysis with a BD FACSCantoII.

Antibodies. The following antibodies were used: anti-C2orf40 (1:100 for immunostaining and immunoblotting; Sigma), which recognizes mouse and rat equally (Fig. S5*A*), anti-RB (1:100; BD Pharmingen), anti-Cyclin D1 (1:1,000; Cell Signaling), anti-Cyclin D2 (1:200; Abcam), anti-Cyclin D3 (1:2,000; Cell Signaling), anti-p27 (1:1,000; Cell Signaling), anti-p16 (1:200; Santa Cruz), anti-BrdU (1:1,000; Hybridoma Bank), anti-GAPDH (1:1,000; Chemicon), anti-Sox2 (1:500; H. Aburatani, Tokyo, Japan), biotinylated anti-Musashi1 (1:500; H. Okano, Japan), anti-NeuN (1:100; Chemicon), anti-Olig1 (1:20; R&D), anti-chondroitin sulfate proteoglycan NG2 (1:100; R&D), anti-O4 (1:3; B. A. Barres, Stanford, CA), anti-Galactocerebroside (GC; hybridoma supernatant, 1:3; ATCC), anti-GFAP (1:500; Dako), and anti-GFP (1:500; Nakalai Tesque). Nuclei were labeled with DAPI (1 μg/mL) or propidium iodide (PI; 1 μg/mL).

RNA Expression Analyses. Total RNA was prepared with the RNeasy Mini Kit (Qiagen) and converted to cDNA using the Transcriptor First Strand cDNA Synthesis Kit (Roche). Gene-specific primers (sequences available on request) were designed using the Primer3 software. RT-PCR was carried out as previously described (37). Quantitative RT-PCR for *Ecrg4* was carried out using SYBR Green 1 Master (Roche) on a LightCycler 480 (Roche) and analyzed with the manufacturer-provided software. *Gapdh* served as the endogenous control for normalization.

Hippocampal NPCs. Hippocampal NPCs were prepared from the adult hippocampus (4-month-old mice) and maintained in serum-free DMEM/F12 medium supplemented with bFGF and EGF (NPC medium) as described previously (38). To examine the function of Ecrg4 in NPCs, the cells were transfected with the m*Ecrg4* expression vector or cultured with rEcrg4, and they were analyzed for SA-β-gal activity and BrdU incorporation as described above. The shRNA experiments were performed in NSC medium with 10% FCS as described above.

MEFs. MEFs were harvested as previously described (39) and maintained in DMEM medium with 10% FCS. The SA-β-gal activity, BrdU incorporation, and *Ecrg4* expression were evaluated at passages 1 and 6. The effects of rEcrg4 on MEFs were examined using the assays described above.

Statistical Analysis. Except as described above for the DNA arrays, Student's *t* test was used for statistical analyses.

ACKNOWLEDGMENTS. We thank Martin Raff, Shigeo Hayashi, and Douglas Sipp for their critical reading of the manuscript and helpful suggestions, Hiroyuki Abratani and Akira Watanabe for providing the Sox2 antibody and the recombinant Sox2 protein, Hirohide Takebayashi for providing the pGEX4T2-mOlig1 vector, Shigekazu Nagata for providing the pEFBOS-EX vector, Hideyuki Okano for providing the biotinylated Musashi1 antibody, Ben A. Barres for providing the O4 hybridoma, Yuka Nakatani for technical assistance, and Takeya Kasukawa and Junko Nishio (RIKEN CDB) for performing the DNA microarray analysis.

1. Kuhn HG, Dickinson-Anson H, Gage FH (1996) Neurogenesis in the dentate gyrus of the adult rat: Age-related decrease of neuronal progenitor proliferation. *J Neurosci* 16:2027–2033.
2. Maslov AY, Barone TA, Plunkett RJ, Pruitt SC (2004) Neural stem cell detection, characterization, and age-related changes in the subventricular zone of mice. *J Neurosci* 24:1726–1733.
3. Molofsky AV, et al. (2006) Increasing p16INK4a expression decreases forebrain progenitors and neurogenesis during ageing. *Nature* 443:448–452.
4. Wolswijk G, Noble M (1989) Identification of an adult-specific glial progenitor cell. *Development* 105:387–400.
5. Rossi F, Cattaneo E (2002) Opinion: Neural stem cell therapy for neurological diseases: Dreams and reality. *Nat Rev Neurosci* 3:401–409.
6. Campisi J (2005) Senescent cells, tumor suppression, and organismal aging: Good citizens, bad neighbors. *Cell* 120:513–522.
7. Campisi J, d'Adda di Fagagna F (2007) Cellular senescence: When bad things happen to good cells. *Nat Rev Mol Cell Biol* 8:729–740.
8. Windrem MS, et al. (2004) Fetal and adult human oligodendrocyte progenitor cell isolates myelinate the congenitally dysmyelinated brain. *Nat Med* 10:93–97.
9. Tang DG, Tokumoto YM, Apperly JA, Lloyd AC, Raff MC (2001) Lack of replicative senescence in cultured rat oligodendrocyte precursor cells. *Science* 291:868–871.
10. Dimri GP, et al. (1995) A biomarker that identifies senescent human cells in culture and in aging skin in vivo. *Proc Natl Acad Sci USA* 92:9363–9367.
11. Kortlever RM, Higgins PJ, Bernards R (2006) Plasminogen activator inhibitor-1 is a critical downstream target of p53 in the induction of replicative senescence. *Nat Cell Biol* 8:877–884.
12. Wajapeyee N, Serra RW, Zhu X, Mahalingam M, Green MR (2008) Oncogenic BRAF induces senescence and apoptosis through pathways mediated by the secreted protein IGFBP7. *Cell* 132:363–374.
13. Yoon YS, Lee JH, Hwang SC, Choi KS, Yoon G (2005) TGF beta1 induces prolonged mitochondrial ROS generation through decreased complex IV activity with senescent arrest in Mv1Lu cells. *Oncogene* 24:1895–1903.
14. Ben-Porath I, Weinberg RA (2004) When cells get stressed: An integrative view of cellular senescence. *J Clin Invest* 113:8–13.
15. Collado M, Serrano M (2006) The power and the promise of oncogene-induced senescence markers. *Nat Rev Cancer* 6:472–476.
16. Lowe SW, Cepero E, Evan G (2004) Intrinsic tumour suppression. *Nature* 432:307–315.
17. Prieur A, Peeper DS (2008) Cellular senescence in vivo: A barrier to tumorigenesis. *Curr Opin Cell Biol* 20:150–155.
18. Su T, Liu H, Lu S (1998) Cloning and identification of cDNA fragments related to human esophageal cancer. *Zhonghua Zhong Liu Za Zhi* 20:254–257.
19. Louis JC, Magal E, Muir D, Manthorpe M, Varon S (1992) CG-4, a new bipotential glial cell line from rat brain, is capable of differentiating in vitro into either mature oligodendrocytes or type-2 astrocytes. *J Neurosci Res* 31:193–204.
20. Santra MK, Wajapeyee N, Green MR (2009) F-box protein FBXO31 mediates cyclin D1 degradation to induce G1 arrest after DNA damage. *Nature* 459:722–725.

21. Nagaya H, et al. (2004) Establishment of a large-scale purification procedure for purified recombinant bovine interferon-tau produced by a silkworm-baculovirus gene expression system. *J Vet Med Sci* 66:1395–1401.
22. Liu Y, Rao MS (2004) Olig genes are expressed in a heterogeneous population of precursor cells in the developing spinal cord. *Glia* 45:67–74.
23. Suh H, et al. (2007) In vivo fate analysis reveals the multipotent and self-renewal capacities of Sox2+ neural stem cells in the adult hippocampus. *Cell Stem Cell* 1: 515–528.
24. Setoguchi T, Kondo T (2004) Nuclear export of OLIG2 in neural stem cells is essential for ciliary neurotrophic factor-induced astrocyte differentiation. *J Cell Biol* 166:963–968.
25. Li J, et al. (2007) A dominant-negative form of mouse SOX2 induces trophectoderm differentiation and progressive polyploidy in mouse embryonic stem cells. *J Biol Chem* 282:19481–19492.
26. Yasuhara N, et al. (2007) Triggering neural differentiation of ES cells by subtype switching of importin-alpha. *Nat Cell Biol* 9:72–79.
27. Gontan C, et al. (2009) Exportin 4 mediates a novel nuclear import pathway for Sox family transcription factors. *J Cell Biol* 185:27–34.
28. D'Angelo MA, Raices M, Panowski SH, Hetzer MW (2009) Age-dependent deterioration of nuclear pore complexes causes a loss of nuclear integrity in postmitotic cells. *Cell* 136: 284–295.
29. Kuilman T, et al. (2008) Oncogene-induced senescence relayed by an interleukin-dependent inflammatory network. *Cell* 133:1019–1031.
30. Kuilman T, Peeper DS (2009) Senescence-messaging secretome: SMS-ing cellular stress. *Nat Rev Cancer* 9:81–94.
31. Allan GJ, Beattie J, Flint DJ (2008) Epithelial injury induces an innate repair mechanism linked to cellular senescence and fibrosis involving IGF-binding protein-5. *J Endocrinol* 199:155–164.
32. Kortlever RM, Bernards R (2006) Senescence, wound healing and cancer: The PAI-1 connection. *Cell Cycle* 5:2697–2703.
33. Untergasser G, et al. (2005) Profiling molecular targets of TGF-beta1 in prostate fibroblast-to-myofibroblast transdifferentiation. *Mech Ageing Dev* 126:59–69.
34. Wang S, Sdrulla A, Johnson JE, Yokota Y, Barres BA (2001) A role for the helix-loop-helix protein Id2 in the control of oligodendrocyte development. *Neuron* 29: 603–614.
35. Smyth GK (2004) Linear models and empirical bayes methods for assessing differential expression in microarray experiments. *Stat Appl Genet Mol Biol* 3: Article 3.
36. Edman LC, et al. (2008) Alpha-chemokines regulate proliferation, neurogenesis, and dopaminergic differentiation of ventral midbrain precursors and neurospheres. *Stem Cells* 26:1891–1900.
37. Kondo T, Raff M (2000) Oligodendrocyte precursor cells reprogrammed to become multipotential CNS stem cells. *Science* 289:1754–1757.
38. Scheel JR, Ray J, Gage FH, Barlow C (2005) Quantitative analysis of gene expression in living adult neural stem cells by gene trapping. *Nat Methods* 2:363–370.
39. Serrano M, Lin AW, McCurrach ME, Beach D, Lowe SW (1997) Oncogenic ras provokes premature cell senescence associated with accumulation of p53 and p16INK4a. *Cell* 88:593–602.